

Excluded Volume Effects in the Quark Meson Coupling Model

P. K. Panda¹, M. E. Bracco², M. Chiapparini², E. Conte² and G. Krein¹

¹ *Instituto de Física Teórica, Universidade Estadual Paulista
Rua Pamplona 145, 01405-900 São Paulo, SP, Brasil*

² *Instituto de Física, Universidade do Estado do Rio de Janeiro
Rua São Francisco Xavier 524, 20559-900, Rio de Janeiro, RJ, Brasil*

Excluded volume effects are incorporated in the quark meson coupling model to take into account in a phenomenological way the hard core repulsion of the nuclear force. The formalism employed is thermodynamically consistent and does not violate causality. The effects of the excluded volume on in-medium nucleon properties and the nuclear matter equation of state are investigated as a function of the size of the hard core. It is found that in-medium nucleon properties are not altered significantly by the excluded volume, even for large hard core radii, and the equation of state becomes stiffer as the size of the hard core increases.

I. INTRODUCTION

The study of the properties of high density and high temperature hadronic matter is of interest for understanding a wide range of phenomena associated with superdense stars [1] and relativistic heavy-ion collisions [2]. One of the open questions in this subject is the correct identification of the appropriate degrees of freedom to describe the different phases of hadronic matter. Although this question will eventually be answered with first-principles calculations with the fundamental theory of the strong interactions quantum chromodynamics (QCD), most probably through lattice QCD simulations, presently one is still far from this goal and, in order to make progress, one must rely on model calculations and make use of the scarce experimental information available. For matter at zero temperature and density close to the saturation density of nuclear matter, experiment seems to indicate that the relevant degrees of freedom are the baryons and mesons. There is a long and successful history of calculations using models based on baryonic and mesonic degrees of freedom, such as potential models [3,4] and relativistic field-theoretical models, generically known as quantum hadrodynamics (QHD) [5,6]. At densities several times larger than the saturation density and/or high temperatures, one expects a phase of deconfined matter whose properties are determined by the internal degrees of freedom of the hadrons. Early studies of deconfined matter [7] used the MIT bag model [8], in which the relevant degrees of freedom are quarks and gluons confined by the vacuum pressure. On the other hand, at high densities, but not asymptotically higher than the saturation density, the situation seems to be very complicated. The complication arises because of the possibility of simultaneous presence of hadrons and deconfined quarks and gluons in the system. Not much progress has been possible in this direction because of the necessity of a model able to describe composites and constituents at the same footing - a step towards this direction is the formalism developed in Ref. [9].

An important step towards the formulation of a model to describe the different phases of hadronic matter in terms of explicit quark-gluon degrees of freedom is the quark-meson coupling (QMC) model, proposed by Guichon [10] some time ago and extensively investigated by Saito, Thomas and collaborators [11] - see also Ref. [12] for related studies. Matter at low density and temperature is described as a system of nonoverlapping bags interacting through effective scalar- and vector-meson degrees of freedom, very much in the same way as in QHD [5,6]. The crucial difference is that in the QMC, the effective mesons couple directly to the quarks in the interior of the baryons, with the consequence that the effective baryon-meson coupling constants become density dependent. In addition, hadronic sizes are explicitly incorporated through form factors calculable within the underlying quark model [13]. At very high density and/or temperature, baryons and mesons dissolve and the entire system of deconfined matter, composed by quarks and gluons, becomes confined within a single MIT bag [7].

The fact that the same underlying quark model is used at different phases of hadronic matter makes the model very attractive conceptually. Many applications and extensions of the model have been made in the last years - see Refs. [13–19] and references therein. Of particular interest for the phenomenology of finite nuclei was the introduction of a density-dependent bag constant by Jin and Jennings [14]. These authors postulated different density dependencies for the bag constant, in a way that the bag constant decreases as the nuclear density increases. One consequence of this is that large values for the scalar and vector mean fields at the saturation density are obtained, leading to spin-orbit splittings of the single-particle levels of finite nuclei that are in better agreement with experiment than those obtained with a density independent bag constant. Another consequence of a smaller bag constant in medium

is that the bag radius becomes considerably larger than in free space [14,16]. At saturation density the nucleon radius increases 25% and at densities three times higher the radius can increase as much as 50%. For higher densities the increase of radius is even more dramatic. The consequences of changing the bag constant for nucleon sizes were investigated by Lu et al. [17].

A large increase of the bag radius naturally raises the question about the validity of the nonoverlapping bag picture that underlies calculations of nuclear matter properties with the model. At normal nuclear matter densities, the average distance between nucleons is of the order of 1.8 fm. Therefore, for densities larger than the normal density and bag radii larger than 1 fm there is a large probability that the bags overlap significantly. However, before concluding that the picture of independent nucleons breaks down, it is important to recall that short-distance correlations are left out in a mean field calculation. These correlations are induced by the combined effects of the Pauli exclusion principle between identical nucleons and the hard-core of the nucleon-nucleon interaction that forbids scattering into occupied levels. The success of the independent particle model of the nuclear shell model is due to the small size of hard core and the Pauli Principle that lead to a “healing” distance of the two nucleon relative wave function that is smaller than the average distance between nucleons in medium [20]. In a model like the QMC, where the finite size of the nucleons is made explicit through a bag structure, the incorporation of this physics in the many-body dynamics is an interesting new development. In the present paper we address this in a phenomenological way through an excluded volume approach. The prescription we use was developed in Ref. [21] for ideal gases and further extended to relativistic field-theoretic models as QHD in Ref. [22]. In this approach, matter in the hadronic phase is described by nonoverlapping rigid spheres, but when the density of matter is such that the relative distance between two spheres becomes smaller than the diameter of the spheres, the excluded volume effect introduces an effective repulsion that mimics the hard-core repulsion of the nucleon-nucleon interaction.

Of course, at very high density the description of hadronic matter in terms of nonoverlapping bags should break down. In a purely geometrical view, one has the picture that once the relative distance between two bags becomes much smaller than the diameter of a bag, quarks and gluons start percolate and individual bags loose their identity. The density for which this starts to happen is presently unknown within QCD. In this respect, it is important not to confuse the bag radius with the radius of the hard-core of the nucleon-nucleon force. Model studies [23] indicate that when the two nucleons start to overlap, medium-range forces are generated from the distortion of the quark distribution. The short-range repulsion, on the other hand, is due to the combined effect of the one-gluon exchange - mainly due to its spin-spin component - and the Pauli exclusion principle between quarks of different nucleons that becomes efficient when the overlap of the two-nucleon wave functions is complete. Although the described scenario might well not be ultimately confirmed by a full QCD calculation, it seems however clear that the two radii, the radius of the MIT bag and the radius of the hard-core of the nucleon-nucleon interaction, are of different sizes and have different origin in the physics of hadron structure. In this sense, the volume of the excluded volume will be taken to be smaller and unrelated to the radius of the underlying MIT bag.

The excluded volume approach we use is thermodynamically consistent. Although the prescription can be extended to take into account Lorentz contraction of the bags [24], in this initial exploratory investigation we use hard-sphere bags, since a complete calculation would lead to massive numerical calculations. In addition, as indicated by the investigations in Ref. [24], the effect of Lorentz contraction is most important for light particles like pions. However, as we will explicitly show, the approach does not lead to violations of causality for the density range where the model makes sense.

The paper is organized as follows. In Section II we present a short review of the excluded volume prescription of Ref. [22] and implement it to the QMC model. Numerical results are presented in Section III and our Conclusions and Perspectives are discussed in Section IV.

II. EXCLUDED VOLUME IN THE QMC MODEL

Initially, for completeness and in order to make the paper selfcontained, we briefly recapitulate the excluded volume prescription of Ref. [22]. Let us start with the ideal gas of one particle species with temperature T , chemical potential μ and volume V . The pressure is related to the grand partition function \mathcal{Z} as

$$P(T, \mu) = \lim_{V \rightarrow \infty} T \frac{\ln \mathcal{Z}(T, \mu, V)}{V}, \quad (1)$$

with \mathcal{Z} defined as

$$\mathcal{Z}(T, \mu, V) = \sum_{N=0}^{\infty} e^{-\mu N/T} Z(T, N, V), \quad (2)$$

where Z is the canonical partition function. The authors in Ref. [22] included the excluded volume effect starting from the canonical partition function as

$$Z^{excl}(T, N, V) = Z(T, N, V - v_0 N) \Theta(V - v_0 N). \quad (3)$$

This ansatz is motivated by considering the volume V for a system of N particles is reduced to an effective volume, $V - v_0 N$ where v_0 is the volume of a particle. In an hadronic gas, v_0 can be interpreted as the region excluded by the hard core of the nucleon-nucleon interaction. For a spherical region, $v_0 = 4\pi r^3/3$ with r the hard-core radius. Using Eq. (3) into Eq. (2), the grand partition function becomes

$$\mathcal{Z}^{excl}(T, \mu, V) = \sum_{N=0}^{\infty} e^{-\mu N/T} Z(T, N, V - v_0 N) \Theta(V - v_0 N). \quad (4)$$

There is a difficulty for evaluation of the sum over N particles in this equation because of the dependence of the available volume on the varying number of particles N because $Z(T, N, V - v_0 N)$ does not factor as a product as in the case of an N -independent volume. To overcome this difficulty the authors in Ref. [22] have performed a Laplace transformation on the variable V in Eq. (4) as

$$\tilde{\mathcal{Z}}^{excl}(T, \mu, \xi) = \int_0^{\infty} dV e^{-\xi V} \mathcal{Z}^{excl}(T, \mu, V). \quad (5)$$

Using Eq. (4) in this, and making the change of variable

$$V = x + v_0 N, \quad (6)$$

one obtains

$$\tilde{\mathcal{Z}}^{excl}(T, \mu, \xi) = \int_0^{\infty} dx e^{-\xi x} \mathcal{Z}(T, \tilde{\mu}, x) = \tilde{\mathcal{Z}}^{excl}(T, \tilde{\mu}, \xi), \quad (7)$$

where $\tilde{\mu} = \mu - v_0 T \xi$. Now the integrand in this is factorizable (for the present case of independent particles) and the sum over N can be implemented. It is a simple exercise [21] to show that the pressure of the system is given as [22]

$$P(T, \mu) = P'(T, \tilde{\mu}), \quad (8)$$

with

$$\tilde{\mu} = \mu - v_0 P(T, \mu). \quad (9)$$

The meaning of Eq. (8) is that the pressure of the system with excluded volume with chemical potential μ , $P(T, \mu)$, is equal to the pressure of a system without excluded volume but with an effective chemical potential $\tilde{\mu} = \mu - v_0 P(T, \mu)$, denoted by $P'(T, \tilde{\mu})$. Note that once the expression for $P'(T, \tilde{\mu})$ is known, the pressure of the system is given by an implicit function.

The baryon density, the entropy density and the energy density for the system are given by the usual thermodynamical expressions

$$\rho(T, \mu) \equiv \left(\frac{\partial P}{\partial \mu} \right)_T = \frac{\rho'(T, \tilde{\mu})}{1 + v_0 \rho'(T, \tilde{\mu})}, \quad (10)$$

$$S(T, \mu) \equiv \left(\frac{\partial P}{\partial T} \right)_\mu = \frac{S'(T, \tilde{\mu})}{1 + v_0 \rho'(T, \tilde{\mu})}, \quad (11)$$

$$\epsilon(T, \mu) \equiv TS - P + \mu \rho = \frac{\epsilon'(T, \tilde{\mu})}{1 + v_0 \rho'(T, \tilde{\mu})}. \quad (12)$$

These relations define a thermodynamical consistent formalism, since the fundamental thermodynamical relations are fulfilled.

Next we apply this formalism to the QMC model for nuclear matter at zero temperature [10,11]. In the QMC model, the nucleon in nuclear matter is assumed to be described by a static MIT bag in which quarks interact with scalar σ_0 and vector ω_0 mean mesonic fields. The mesonic fields are meant to represent effective degrees of freedom,

not necessarily identified with real mesons. Therefore, since the introduction of the excluded volume is to represent the hard core nucleon-nucleon interaction, Eqs. (8)-(12) will be applied to the baryons only. The same prescription has been used in the application of the formalism to QHD in Ref. [22].

In the QMC model, the pressure and energy density receive contributions from baryons and mesons and are given as

$$P = P_B - \frac{1}{2}m_\sigma^2\sigma_0^2 + \frac{1}{2}m_\omega^2\omega_0^2, \quad (13)$$

$$\epsilon = \epsilon_B + \frac{1}{2}m_\sigma^2\sigma_0^2 + \frac{1}{2}m_\omega^2\omega_0^2, \quad (14)$$

where P_B and ϵ_B are the baryon contributions. As said above, the excluded volume will be applied only to the baryonic contributions and, at zero temperature, one needs to consider only Eqs. (10) and (12),

$$\rho = \frac{\rho'}{1 + v_0\rho'}, \quad (15)$$

$$\epsilon_B = \frac{\epsilon'_B}{1 + v_0\rho'}. \quad (16)$$

For practical calculations, it is convenient to parameterize ρ' in terms of a k_F according to

$$\rho' = \frac{\gamma}{6\pi^2} k_F^3. \quad (17)$$

This allows to write the QMC expressions for P'_B and ϵ'_B as

$$P'_B = \frac{1}{3} \frac{\gamma}{2\pi^2} \left[\frac{1}{4} k_F^3 \sqrt{k_F^2 + M^{*2}} - \frac{3}{8} M^{*2} k_F \sqrt{k_F^2 + M^{*2}} + \frac{3}{8} M^{*4} \ln \left(\frac{k_F + \sqrt{k_F^2 + M^{*2}}}{M^*} \right) \right], \quad (18)$$

$$\epsilon'_B = \rho' \sqrt{k_F^2 + M^{*2}} - P'_B. \quad (19)$$

In these, M^* is the in medium nucleon mass calculated with the MIT bag. Its value is determined by solving the MIT bag equations for quarks coupled to the mean fields σ_0 and ω_0 . In order to completely determine M^* , and therefore the nuclear matter properties Eqs. (15) and (16), one needs σ_0 and ω_0 . The scalar mean field is determined selfconsistently from the minimization condition at density ρ :

$$\frac{\partial \epsilon}{\partial \sigma_0} = 0, \quad (20)$$

which leads to

$$\sigma_0 = \frac{1}{1 + v_0\rho'} \frac{\Sigma(\sigma_0)}{m_\sigma^2}, \quad (21)$$

with

$$\Sigma(\sigma_0) = -\frac{1}{\pi^2} \frac{\partial M^*}{\partial \sigma_0} \left[k_F \sqrt{k_F^2 + M^{*2}} - M^{*2} \ln \left(\frac{k_F + \sqrt{k_F^2 + M^{*2}}}{M^*} \right) \right]. \quad (22)$$

The vector mean field ω_0 is obtained from its equation of motion as

$$\omega_0 = \frac{3g_\omega^q}{m_\omega^2} \rho. \quad (23)$$

Solution of Eq. (21) proceeds as follows. For a given ρ , we use Eq. (15) to obtain ρ' , and from this ρ' we obtain k_F of Eq. (17). The derivative $\partial M^*/\partial \sigma_0$ can be done explicitly, $\Sigma(\sigma_0)$ is then known, and the transcendental equation for σ_0 is easily solved numerically. The results are presented in the next section.

III. RESULTS AND DISCUSSIONS

We start fixing the free-space bag properties. We use zero quark masses only and use two values for the bag radius, $R = 0.6$ fm and $R = 0.8$ fm. There are two unknowns, z_0 and the bag constant B . These are obtained as usual by fitting the nucleon mass $M = 939$ MeV and enforcing the stability condition for the bag. The values obtained for z_0 and B are displayed in Table 1.

Next we proceed to nuclear matter properties. We will consider two versions of the model. In the first one, the bag constant B is fixed at its vacuum value, and in the second one the bag constant changes accordingly to the original Jin and Jennings [14] ansatz, namely

$$B^* = B \exp\left(-\frac{4g_\sigma^B \sigma}{M_N}\right), \quad (24)$$

where g_σ^B is an additional parameter and B is the value of the bag constant in vacuum. In this work we use $g_\sigma^B = 2.8$, which is the same as in Ref. [17].

The quark-meson coupling constants g_σ^q and $g_\omega = 3g_\omega^q$ are fitted to obtain the correct saturation properties of nuclear matter, $E_B \equiv E/A - M = \epsilon/\rho - M = -15.7$ MeV at $\rho = \rho_0 = 0.15$ fm⁻³. We take the standard values for the meson masses, $m_\sigma = 550$ MeV and $m_\omega = 783$ MeV. We present results for three different values of the hard core, $r = 0.4$ fm, 0.5 fm and 0.6 fm, and for two values of bag radii, $R = 0.6$ fm and 0.8 fm. The pair $r = 0.6$ fm, $R = 0.6$ fm represents the situation that the size of the hard-core is the same as of the bag and is included for illustrative purposes.

Initially, we investigate the effect of the excluded volume on the binding energy per particle for the values of r and R mentioned above. The results for the different values of r and R and shown in Fig. 1, where we plot E_B as a function of the nuclear density ρ . In this figure the coupling constants g_σ^q and g_ω for a given R are the same for the different values of r . As expected, the effect of an effective repulsion due to the hard core is clearly seen in this figure. The effect obviously increases as the size of hard-core increases. At the saturation density, the largest value of the effective repulsion is of the order of 4 MeV. The effect is not as dramatic as one could expect. For comparison with another repulsive effect, we mention that Fock terms [13] give 5 MeV repulsion for the binding energy.

We now readjust the coupling constants g_σ^q and g_ω such as to obtain the correct saturation binding energy of nuclear matter for the different values of r and R . Our aim is to investigate the changes on the properties of nuclear matter and in-medium nucleon properties due to the hard core. Tables II and III present the values of the coupling constants and the ratios of in-medium to free-space bag radii R^*/R , nucleon masses M^*/M and bag eigenvalues x^*/x . The Tables also show the changes in the incompressibility for different hard core radii. The results are such that nucleon properties are not changed significantly, being at most at the level of 2%. The incompressibility is a little more sensitive than nucleon properties to the extra repulsion induced by the hard core, but the increase is at most 120 MeV.

The effect of the hard core as a function of the nuclear density ρ on the binding energy is shown in Figure 2. One notices that the equation of state becomes stiffer as the size of the hard core increases. The ratios R^*/R , M^*/M and the σ_0 field as functions of ρ are shown in Figures 4, 5 and 6, respectively. As found previously, the in-medium bag radius decreases (increases) for a constant (in-medium changed) bag parameter. Now, the change in the in-medium bag radius decreases as the hard core radius increases. This is clearly an effect due to the fact that as the hard core radius increases, one has less attraction, and the bag properties change less. In Fig. 5 one sees the interesting feature that as the in-medium nucleon mass increases, the binding energy curve is stiffer when volume corrections are included, contrary to the case without excluded volume. This is again an effect of extra repulsion due to the hard core. That one gets less attraction as the hard core radius increases can be seen in Figure 6, where we plot σ_0 as function of ρ for different combinations of r and R . The less attraction is simply due to the factor $1 + v_0\rho$ in the denominator in Eq. (21), which increases as v_0 increases and makes the r.h.s. of Eq. (21) to contribute less to σ_0 .

To conclude this section, we mention that for neutron stars, for instance, one is interested in the equation of state pressure P versus energy ϵ . One important question here is to check whether causality is respected by such an equation of state. Figure 3 presents P versus ϵ for different values of r and R . For comparison, the causal limit $P = \epsilon$ is also shown in the figure. Clearly seen is that all the cases studied here respect the causal condition $\partial P/\partial\epsilon \leq 1$, so that the speed of sound remains lower than the speed of light. This result is consistent with Ref. [25], where it was shown that for realistic situations of temperatures below the QCD phase transition, which is believed to be of the order of 200 MeV, the excluded volume prescription used here [21,22] does not lead to conflicts with causality.

IV. CONCLUSIONS AND PERSPECTIVES

In this paper we have incorporated excluded volume effects in the quark meson coupling model in a thermodynamically consistent manner. The excluded volume simulates in a phenomenological way the short range hard-core repulsion of the nucleon-nucleon force, in the sense it does not allow nucleons to occupy all space as they were point-like. The consequences for in-medium nucleon properties and saturation properties of nuclear matter due to the excluded volume effects have been investigated for different bag and hard core radii. The bag constant was allowed to change in medium and differences with respect to a fixed bag constant were studied. It was also shown that the prescription used does not lead to violations of causality.

We found that the excluded volume induces an effective repulsion that increases as the size of hard-core increases. The repulsion is at most 4 MeV at the saturation density. In-medium nucleon properties, such as bag radius and nucleon mass are not changed significantly, as compared to the changes when excluded volume effects are not taken into account. The changes are at most at the level of 2%. The incompressibility is a little more sensitive, but the increase is at most 120 MeV. The excluded volume also induces the effect that the binding energy curve as a function of the nuclear density is stiffer as the in-medium nucleon mass increases. This feature is contrary to the case without excluded volume. It arises because of the extra repulsion due to the hard core that leads to a smaller sigma field and consequently to less attraction.

The formalism of the present paper can be extended in several ways. We intend to incorporate taking into account of the Lorentz contraction of the bags. As indicated by the authors of Ref. [24], the effects of the Lorentz contraction is most important for light particles like pions. Also possible extensions of the formalism presented here to finite temperatures are currently under progress. As a final remark, it should be clear that an excluded volume approach is by no means a complete replacement of explicit calculations of short-range correlation effects, such as through a Bethe-Goldstone-type of approach [20]. There is one attempt to include short-range quark-quark correlations in the QMC model [26] and its further investigation in the context of a Bethe-Goldstone approach is an interesting new direction that should be undertaken in the near future.

V. ACKNOWLEDGMENTS

One of the author (PKP) would like to acknowledge the IFT, São Paulo, for kind hospitality. This research has been supported in parts by CNPq and FAPESP (grant 99/08544-0).

-
- [1] H. Heiselberg and V. Pandharipande, *Ann. Rev. Nucl. Part. Sci.* **50**, 481 (2000).
 - [2] J.W. Harris and B. Müller, *Ann. Rev. Nucl. Part. Sci.* **46**, 71 (1996).
 - [3] B. Friedman and V.R. Pandharipande, *Nucl. Phys.* **A361**, 502 (1981).
 - [4] R.B. Wiringa, V. Fiks, and A. Fabrocini, *Phys. Rev. C* **38**, 1010 (1988).
 - [5] J.D. Walecka, *Ann. of Phys.* **83**, 491 (1974); B.D. Serot and J.D. Walecka, *Int. J. Mod. Phys. E* **6**, 515 (1997).
 - [6] R.J. Furnstahl, B.D. Serot and H.B. Tang, *Nucl. Phys.* **A615**, 441 (1997); H. Mueller and B.D. Serot, *Nucl. Phys.* **A606**, 508 (1996).
 - [7] J.C. Collins and M.J. Perry, *Phys. Rev. Lett.* **34**, 1353 (1975); G. Baym and S.A. Chin, *Phys. Lett. B* **62**, 241 (1976); B.D. Keister and L.S. Kisslinger, *Phys. Lett. B* **64**, 117 (1976); G. Chapline and M. Nauenberg, *Phys. Rev. D* **16**, 450 (1977); B. Freedman and L. McLerran, *Phys. Rev. D* **17**, 1109 (1978).
 - [8] A. Chodos, R.L. Jaffe, K. Johnson, C.B. Thorn, and V. Weisskopf, *Phys. Rev. D* **9**, (1974) 3471; A. Chodos, R.L. Jaffe, K. Johnson, and C.B. Thorn, *Phys. Rev. D* **10**, 2599 (1974).
 - [9] D. Hadjimichef, G. Krein, S. Szpigiel, and J.S. da Viegua, *Ann. Phys. (N.Y.)* **268**, 105 (1998).
 - [10] P. A. M. Guichon, *Phys. Lett. B* **200**, 235 (1988).
 - [11] K. Saito and A.W. Thomas, *Phys. Lett. B* **327**, 9 (1994); **335**, 17 (1994); **363**, 157 (1995); *Phys. Rev. C* **52**, 2789 (1995); P.A.M. Guichon, K. Saito, E. Rodionov, and A.W. Thomas, *Nucl. Phys.* **A601** 349 (1996); K. Saito, K. Tsushima, and A.W. Thomas, *Nucl. Phys.* **A609**, 339 (1996); *Phys. Rev. C* **55**, 2637 (1997); *Phys. Lett. B* **406**, 287 (1997); K. Tsushima, K. Saito, J. Haidenbauer, and A. W. Thomas, *Nucl. Phys. A* **630**, 691 (1998).
 - [12] T. Frederico, B.V. Carlson, R.A. Rego, and M.S. Hussein, *J. Phys. G* **15**, 397 (1989); S. Fleck, W. Bentz, K. Shimizu, K. Yazaki, *Nucl. Phys. A* **510**, 731 (1990); E. Naar, M.C. Birse, *J. Phys. G* **19**, 555 (1993).

- [13] G. Krein, A.W. Thomas, and K. Tsushima, Nucl. Phys. A **650**, 313 (1999); M.E. Bracco, G. Krein, and M. Nielsen, Phys. Lett. B **432** 258 (1998).
- [14] X. Jin and B.K. Jennings, Phys. Lett. B **374**, 13 (1996); Phys. Rev. C **54**, 1427 (1996).
- [15] P. G. Blunden and G.A. Miller, Phys. Rev. C **54**, 359 (1996); G. Krein, D.P. Menezes, M. Nielsen, and C. Providencia, Nucl. Phys. **A674**, 125 (2000); N. Barnea and T.S. Walhout, Nucl. Phys. **A677**, 367 (2000); H. Shen and H. Toki, Phys. Rev. C **61**, 045205 (2000).
- [16] S. Pal, M. Hanauske, I. Zakout, H. Stöcker, and W. Greiner, Phys. Rev. C **60**, 015802 (1999).
- [17] D.H. Lu, K. Tsushima, A.W. Thomas, A.G. Williams and K. Saito, Nucl. Phys. **A634**, 443 (1998).
- [18] P.K. Panda, A. Mishra, J.M. Eisenberg, W. Greiner, Phys. Rev. C **56**, 3134 (1997); I. Zakout, H.R. Jaqaman, S. Pal, H. Stöcker, and W. Greiner, Phys. Rev. C **61**, 055208 (2000).
- [19] P.K. Panda, R. Sahu, C. Das, Phys. Rev. C **60**, 38801 (1999).
- [20] L.C. Gomes, J.D. Walecka and V.F. Weisskopf, Ann. Phys. (N.Y.) **3**, 241 (1958); J.D. Walecka and L.C. Gomes, Ann. da Acad. Brasileira de Ciências **39**, 361 (1967).
- [21] M.I. Gorenstein, V.K. Petrov, and G.M. Zinovjev, Phys. Lett. B **106**, 327 (1981).
- [22] D.H. Rischke, M.I. Gorenstein, H. Stöcker and W. Greiner, Z. Phys. C **51**, 485 (1991); B.Q. Ma, Q.R. Zhang, D.H. Rischke and W. Greiner, Phys. Lett. B **315**, 29 (1993).
- [23] T. Goldman and G. J. Stephenson, Jr., Phys. Lett. B **146**, 143 (1984); T. Goldman, G. J. Stephenson, Jr., and K. E. Schmidt, Nucl. Phys. A **481**, 621 (1988); Fang Wang, Guang-han Wu, Teng, L.J. , and T. Goldman, Phys. Rev. Lett. **69**, 2901 (1992); T. Goldman, K. Maltmann, and G. J. Stephenson, Jr., Phys. Lett. B **324**, 1 (1994); Guang-han, Jia-Lun Ping, Li-jian Teng, Fan Wang, and T. Goldman, Nucl. Phys. A **673**, 279 (2000).
- [24] K.A. Bugaev, M.I. Gorenstein, H. Stöcker, and W. Greiner, Phys. Lett. B **485**, 121 (2000).
- [25] N. Prasad, K.K. Singh, and C.P. Singh, Phys. Rev. C **62**, 037903 (2000).
- [26] K. Saito and K. Tsushima, Prog. Theor. Phys. (Kyoto) **105**, 373 (2001).

TABLE I. Parameters used in the calculation.

m_q (MeV)	R (fm)	$B^{1/4}$ (MeV)	z_0	m_σ (MeV)	m_ω (MeV)
0	0.6	211.3	3.987	550	783
0	0.8	170.3	3.273	550	783

TABLE II. quark-sigma and omega-nucleon are used for different cases in our calculation for $R = 0.6$ fm. Effective nucleon radius, effective mass, bag eigen value and compressibility are given for different sets at the saturation density. Note that hard-core radius $r = 0$ fm corresponds to normal QMC model

	Hard-core radius (fm)	g_s^q	g_ω	R^*/R	M^*/M_N	x^*/x	K MeV
$B=\text{constant}$	0	5.98	8.95	0.9934	0.7757	0.8659	257
	0.4	5.93	8.81	0.9936	0.7789	0.8684	285
	0.5	5.87	8.66	0.9939	0.7824	0.8711	316
	0.6	5.76	8.38	0.9942	0.7887	0.8759	372
$B = B^*$	0	4.32	9.87	1.0849	0.7388	0.8882	268
	0.4	4.26	9.72	1.0844	0.7426	0.8909	297
	0.5	4.20	9.57	1.0839	0.7468	0.8938	330
	0.6	4.09	9.29	1.0830	0.7543	0.8988	386

TABLE III. Same as Table II for $R = 0.8$ fm

	Hard-core radius (fm)	g_s^q	g_ω	R^*/R	M^*/M_N	x^*/x	K MeV
$B=\text{constant}$	0	5.74	8.19	0.9930	0.8034	0.8342	249
	0.4	5.69	8.06	0.9932	0.8060	0.8371	277
	0.5	5.64	7.91	0.9935	0.8088	0.8404	307
	0.6	5.54	7.64	0.9938	0.8139	0.8461	361
$B = B^*$	0	4.14	9.34	1.0799	0.7609	0.8594	261
	0.4	4.09	9.20	1.0795	0.7640	0.8627	290
	0.5	4.03	9.05	1.0792	0.7675	0.8661	322
	0.6	3.93	8.79	1.0785	0.7737	0.8723	378

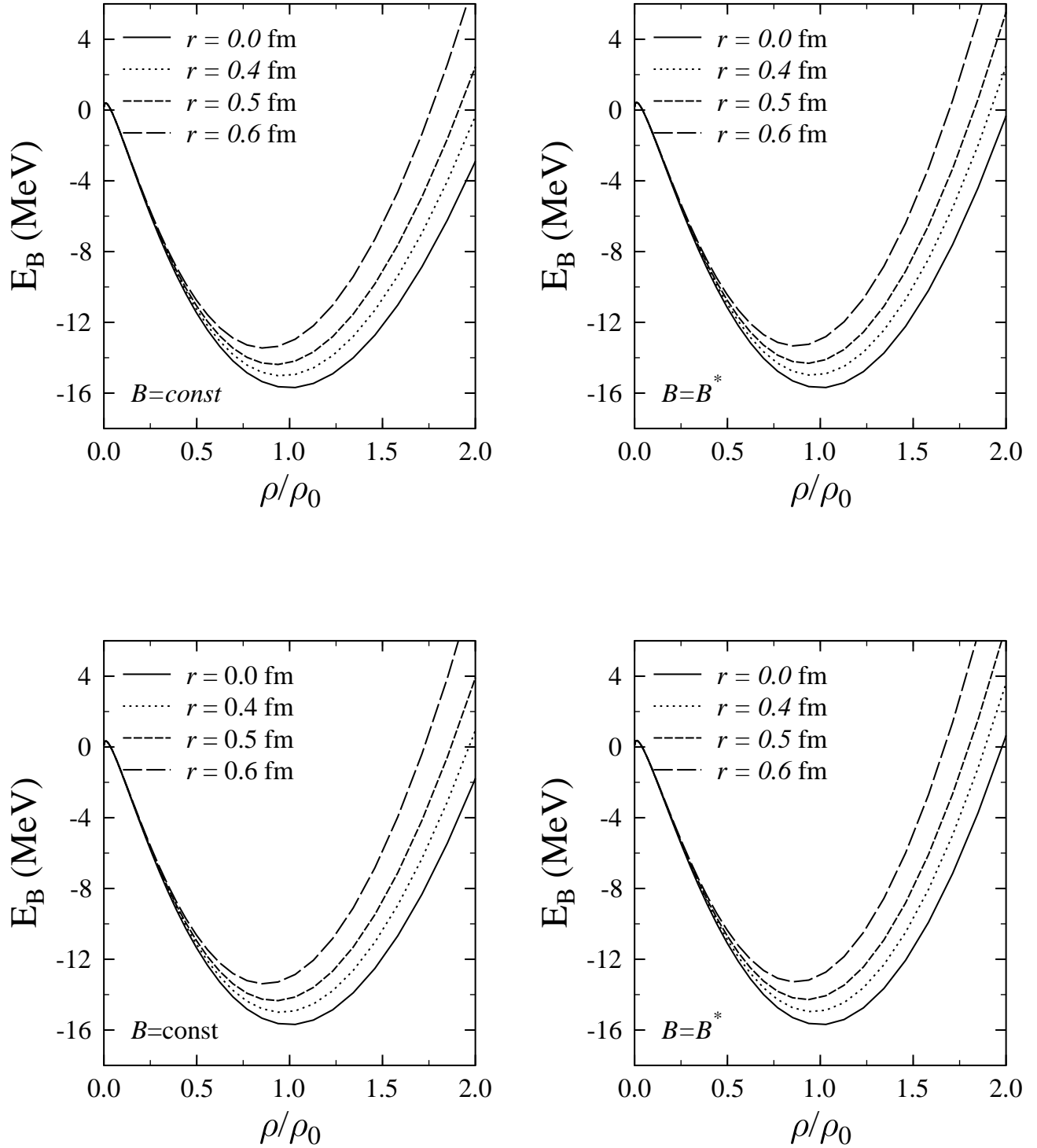


FIG. 1. The energy per nucleon of nuclear matter as a function of ρ/ρ_0 for different hard-core radii. All curves are for the same set of quark-meson coupling constants. The upper panel of the figure corresponds to $R = 0.8$ fm and the lower one is for $R = 0.6$ fm.

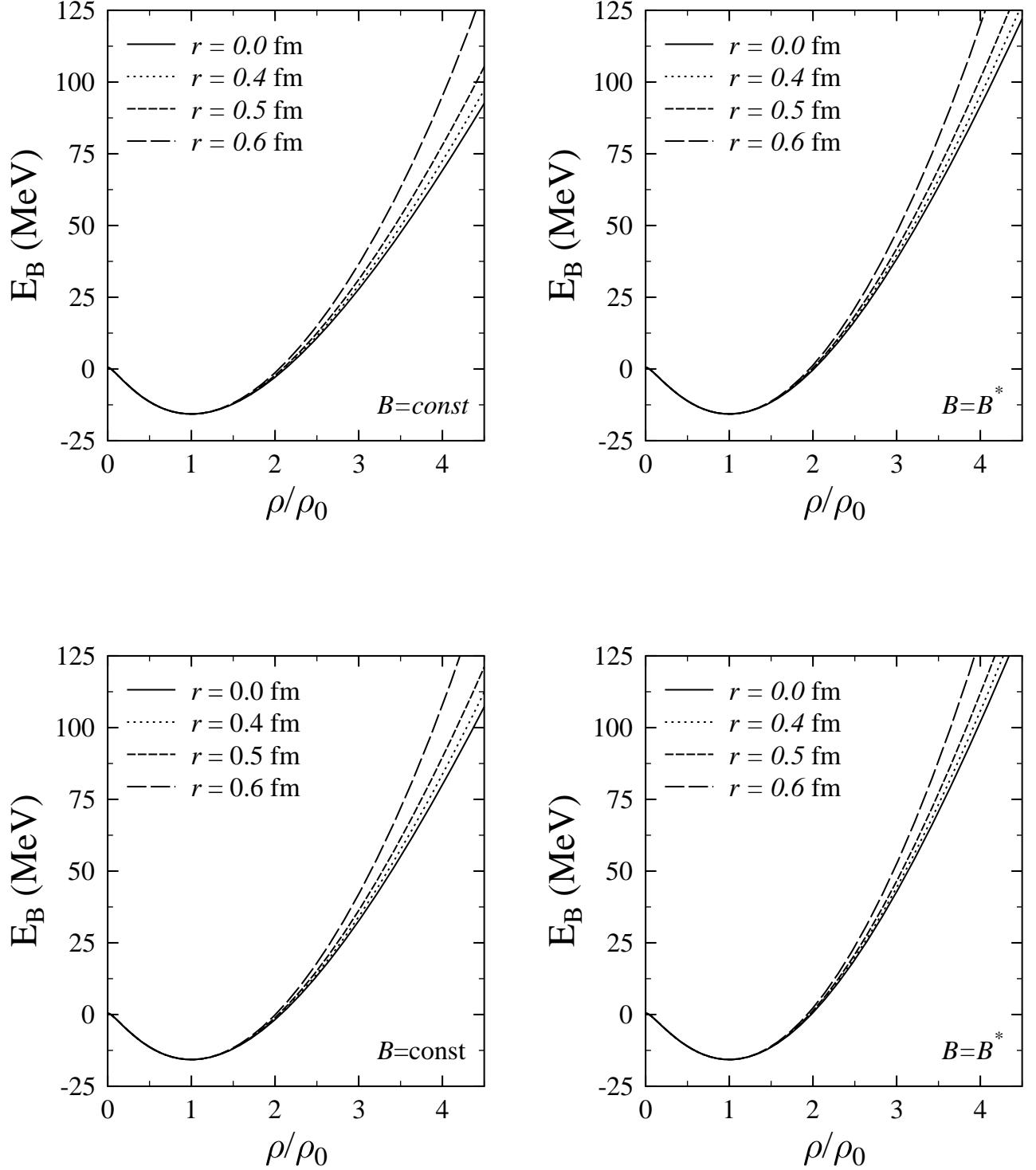


FIG. 2. The energy per nucleon of nuclear matter as a function of ρ/ρ_0 for different hard-core radii. The quark-meson coupling constants are refitted such as to obtain the correct saturation point. The upper panel of the figure corresponds to $R = 0.8$ fm and the lower one is for $R = 0.6$ fm.

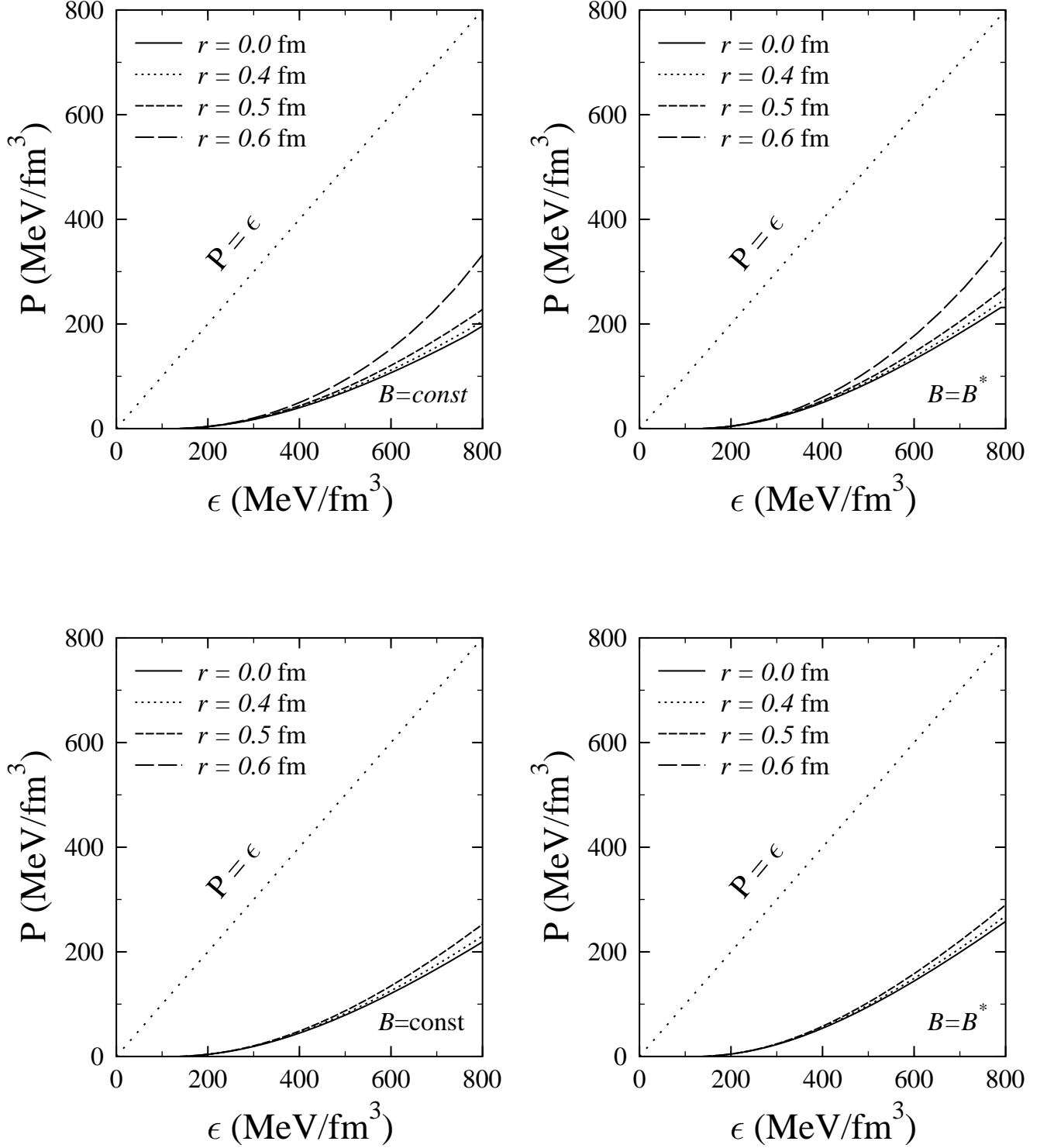


FIG. 3. The pressure of the nuclear matter as a function of the energy density corresponding to the different hard-core radii. The upper panel of the figure corresponds to $R = 0.8 \text{ fm}$ and the lower one is for $R = 0.6 \text{ fm}$.

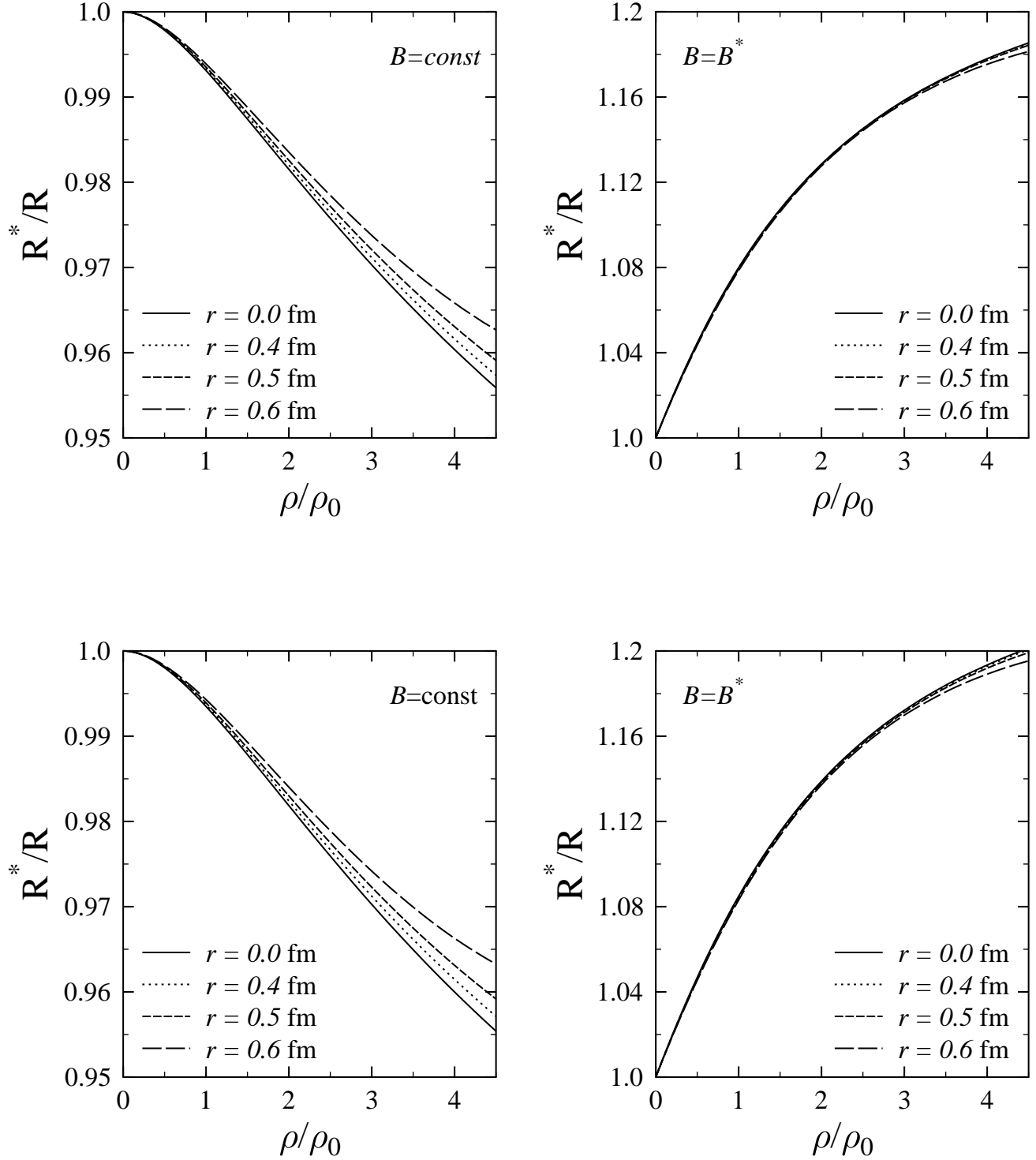


FIG. 4. The effective radius of the nucleon as a function of ρ/ρ_0 corresponding to the different hard-core radii. The upper pannel of the figure corresponds to $R = 0.8$ fm and the lower one is for $R = 0.6$ fm.

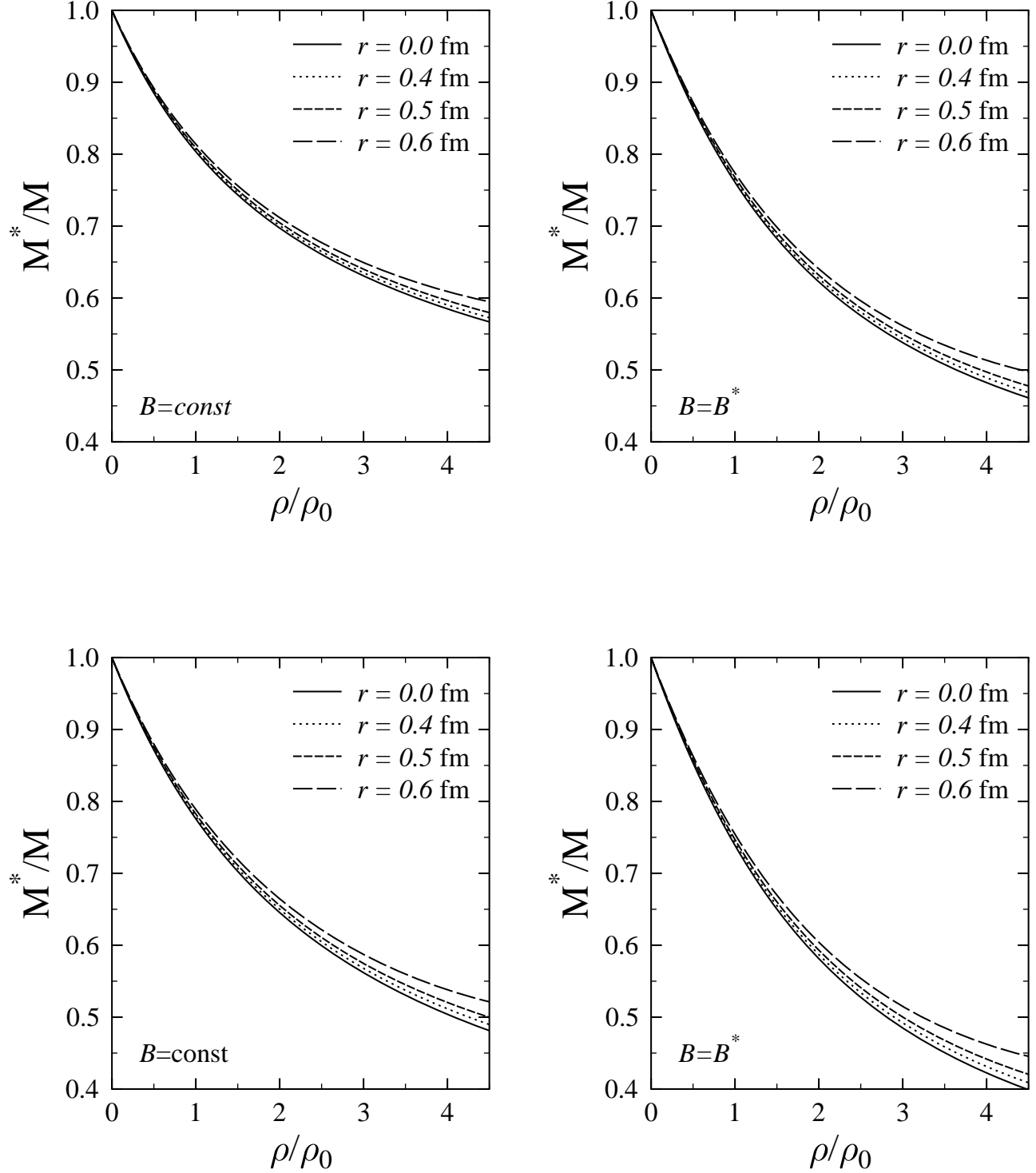


FIG. 5. The in-medium nucleon mass as a function of ρ/ρ_0 corresponding to the different hard-core radii. The upper panel of the figure corresponds to $R = 0.8$ fm and the lower one is for $R = 0.6$ fm.

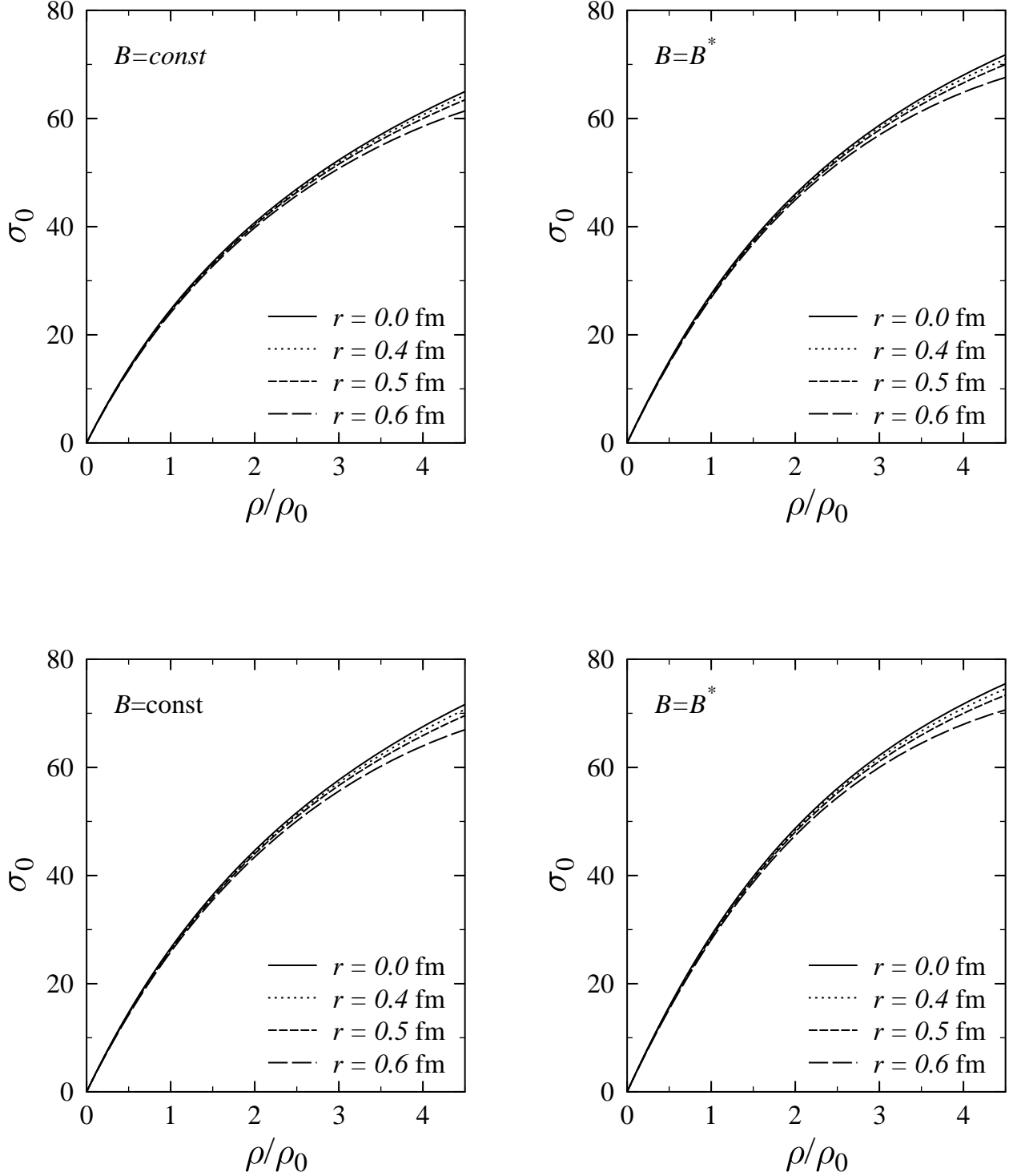


FIG. 6. The sigma field as a function of ρ/ρ_0 corresponding to the different hard-core radius. The upper panel of the figure corresponds to $R = 0.8$ fm and the lower one is for $R = 0.6$ fm.